



Energy Performance Analysis of Solar-wind Catchers Under Hot and Dry Climatic Condition in Iran-Yazd

Hedayat^{a,*}, Z., Samkhanian^b, N., Belmans^a, B., Ayatollahi^c, M.H., Wouters^a, I., Descamps^a, F.

^aDept. of Architectural Engineering, Vrije Universiteit Brussel, Belgium.

*E-Mail: Zhaleh.Hedayat@vub.ac.be

^bDept. of Mechanical Engineering, Tarbiat modares University, Iran.

^cDept. of Architecture, Yazd University, Iran.

ARTICLE INFO

Received: 27 September 2016
Received in revised form: 29 December 2016
Accepted: 30 December 2016

Keywords:

Solar-Wind catcher;
long-term experimental dataset; Yazd city; Iran

A B S T R A C T

Ancient wind catchers of Yazd city as net zero energy building components request the detailed numerical and experimental studies to renovate and reuse in old part of the city and for developing the new design strategies in future. In this ingenious natural ventilation strategy no other energy sources are required except wind and sun. In this research, the effect of both wind and sun on the flow and thermal behaviour of the solar-wind catchers of Yazd city - a city with very high solar radiation - in Iran, are investigated numerically and experimentally. This paper represents a systematic evaluation of isothermal 3D CFD modelling for predicting mean air velocity distributions over and through the wind catcher at three reference wind directions of 330°, 90° and 150°, using Open source CFD package (OpenFOAM). The evaluation is based on a grid-sensitivity analysis and on validation with full scaled long term measurement data set. The validated CFD simulation results show that steady RANS with Standard $k-\epsilon$ model, in spite of its limitations, can accurately predict the flow behaviour of wind catchers at wind direction of 90° with the average deviations of 19%, which is considered a good agreement against the long term experimental results. Moreover the thermal behaviour of wind catcher during a summer day is discussed. The study reveals that the solar wind catchers of Yazd city, is quite effective in lowering air temperature and enhancing air circulation through the buildings. The result of this study will be useful for designing solar-wind catchers under hot and dry climate conditions.

© 2017 Published by University of Tehran Press. All rights reserved.

1. Introduction

Wind catchers of Yazd city in Iran so called Baud-Geers in Persian, extract and supply air into the buildings using ventilation principles of stack ventilation and wind-induced ventilation, respectively. In this ingenious natural ventilation strategy no other energy sources are required except wind and sun. In hot and dry regions, the impact of solar radiation on wind catcher performance is higher comparing to the other regions.

Many researchers have been studied the functional behavior of the wind towers in Iran. Bahadori [2], performed full analysis of the design of wind towers in several locations such as Yazd city and presented two new designs of wind towers. Yaghubi M.A, 1991 studied a thermal performance of three naturally ventilated building linked to the wind tower. A short-term experimental study is conducted to analyze the wind towers performance [20]. Montazeri [13] also investigated the effects of the numbers of openings by modeling a circular cross section wind tower that has several openings at equal angles. In this research, the wind and sun energy performance analysis of the solar-wind catchers of Yazd city - a city with very high solar radiation - in Iran, are

investigated experimentally and numerically. Hence, in present study the effect of both sun and wind simultaneously is considered when evaluating the performance of the wind catcher system using numerical simulation, long term and short term experimental dataset.

2. Material and Method

For numerical simulation and to study the whole image of the flow field and the airflow pattern around and inside the wind-induced natural ventilation wind towers of Yazd city, a reference case study is selected at the old city center of Yazd. The model of experimental house with wind tower is built and used in the open source CFD package (OpenFOAM) for simulation. Figure 1 shows the model of the experimental house linked to the wind tower. The isothermal simulation results are used to validate against the long-term empirical measurement results.

For the experimental study and evaluation of thermal behavior of wind catcher, a short term experimental data of the warmest day of measuring period was selected. All required data of wind and temperature was stored in sub-hourly timescale. A mean average hourly data was used to

look at the daily wind and solar pattern during a summer day.

1. The measurements data set and the template CFD model of this research are intended to support and used in future studies on performance analysis of the other wind catchers of Yazd and, this way, to contribute to improved solar -wind catcher design in future.

3. Experimental Measurements

A representative four-sided wind catcher in the historic city center of Yazd was selected to equip with temperature, wind, air velocity and solar sensors. The monitoring was performed during 2014-2015 [10, 11,12].

Based on the literature review, on-site measurements should be made to provide validation data for the CFD simulations [6, 17]. The on-site measurements, in spite of their disadvantages, represent the complex reality without simplifications and are therefore the true validation data for numerical models. It is however important that these measurement are made during a sufficiently long measurement period. To establish a long-term dataset on a full scale wind tower the outdoor wind speed and the air velocities in four tower shafts of the experimental house (Mortaz house) wind catcher in city campus of Yazd university, were monitored during a full year monitoring campaign in 2014-2015.

In this study a yearly and daily pattern of climate dataset were used for the CFD validation purposes and thermal analysis of the wind catcher performance.

3.1. O-site data measurements

A local weather station was installed to obtain the outdoor wind and temperature data of the site. Wind measuring equipment at the weather station was located at a height of 10m above ground level. For the duration of 1 year, the data was filtered in case of sensor malfunction, missing data and other typical errors [AWS 1997]. For CFD validation purposes the wind data were carefully analyzed in view of selecting the yearly prevailing wind directions over the year which can be more effective to analyze the performance of wind catcher. Three prevailing wind directions of east, south-east and north-west were identified which the mean air velocities were computed for the different tower shafts.

Apart from the experimental wind data measurement, it is important to gain information on the type of wind activity which is present at the location and from which direction the wind is predominant, so that the reference wind velocity could be specified in the CFD model at the inlet boundaries. All these information were obtained from wind data recorded at the Yazd meteorological station, which is the nearest weather station.

3.2. Indoor data measurements

Indoor air velocity measurements in four tower shafts have been performed using four air velocity sensors (A4 – A1 – A2 – A3) with the working range of 0-20 m/s were installed in the middle of four tower shafts (shaft A – B – D – E) in height of 2.00 m above the outlet of the tower. A long-term measurement has been conducted during 2014-2015.

4. CFD simulation: process and results

In CFD simulations, a large number of choices have to be made by the user. These choices can have a very large impact on the simulation results. In a typical CFD simulation, the user has to choose the approximate equations describing the flow (steady RANS, unsteady RANS (URANS), LES or hybrid URANS/LES), the level of detail in the geometrical representation of the buildings, the size of the computational domain, the type and resolution of the computational grid, the boundary conditions, the discretization schemes, the initialization data and the iterative convergence criteria. Important best practice guidelines have been developed and/or published by many researchers [4,5, 6, 15, 16, 17]. In this section, the CFD simulation parameters are briefly outlined:

3.1. Computational geometry and grid

A computational model was made of the full scale building model linked to the wind tower used for the on-site measurements. The dimensions of the computational domain were chosen based on the best practice guidelines by Franke et al. [7]. The upstream domain length is $5H = 70$ m. The resulting dimensions of the domain were $W \times D \times H = 500 \times 500 \times 80$ m³. The computational grid was created using the blockMesh and snappyHexMesh utilities in OpenFOAM resulting in a hybrid grid with 4,294,876 polyhedral and hexahedral cells. Two refinement boxes control the cells located in the immediate surroundings of the building model and the tower model. 17 and 10 cells are used along the width and depth of the each tower shafts, respectively, as shown in Figure.1 The minimum and maximum cell volumes in the domain are approximately 3.15×10^{-6} m³ and 3683.49 m³, respectively.

The distance from the center point of the wall adjacent cell to the wall, for the wind-catcher and ground plane is 23.19 m and 221 m respectively. This corresponds to y^+ values between 20 and 350. As standard wall functions are used in this study, these values ensure that the centre point of the wall-adjacent cell is placed in the logarithmic layer. The domain shape and size (figure.1) allows modelling different wind directions 330° , 90° and 150° corresponding to the prevailing wind directions from experimental measurement.

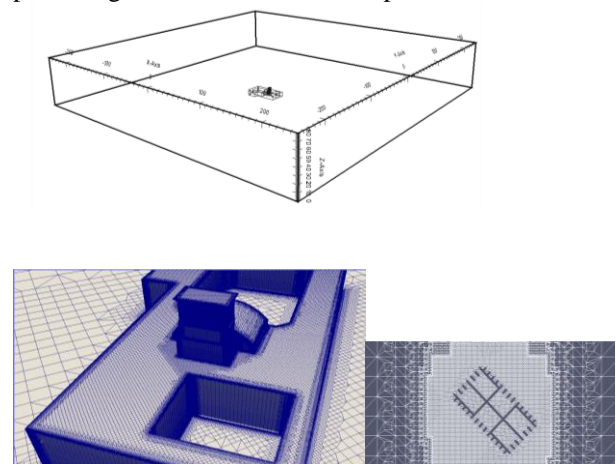


Figure 1. (top) Computational domain. (bottom-left) Grid at building surfaces. (bottom-right) Detail of grid near and inside wind tower shafts.

4.2. Boundary conditions

The atmospheric boundary layer inflow at the inlet of the domain consists of the profiles of mean wind speed, turbulent kinetic energy and turbulence dissipation rate [15]. The mean wind speed profile is prescribed by the logarithmic law with z_0 according to the average building height ($h=7$ m, $z_0 = 0.7$ m). Based on the meteorological data, the reference wind speed is different in different wind directions e.g. $U_{ref} = 5.5$ m/s at 10 m height for wind direction of 90° . The ABL profile is derived from the friction velocity, flow direction and the direction of the parabolic coordinate. (figure2)

(1)

$$U(z) = \frac{U_{*a}}{\kappa} \ln\left(\frac{z+z_0}{z_0}\right)$$

where U^* is the frictional velocity, K is Karman's constant, z the vertical coordinate [m], z_0 is the surface roughness length [m] and z_g as minimum value in z direction [m].

In the simulations the inlet boundary conditions (mean velocity U , turbulent kinetic energy k and turbulence dissipation rate ϵ) were based on the measured incident vertical profiles of mean wind speed U and longitudinal turbulence intensity I_u (figure. 2) The turbulent kinetic energy k was calculated from U and I_u using Eq. (1), where a is a parameter in the range between 0.5 and 1.5 [2,3]., the turbulence kinetic energy with the $a=1.5$ is chosen. The turbulence dissipation rate ϵ with the von Karman constant ($=0.41$) are given by Eq. (2).

(2)

$$k(z) = a(I_u(z)u(z))^2$$

$$\epsilon(z) = \frac{u_{ABL}^{*3}}{\kappa(z+z_0)}$$

At the outlet, zero static pressure is specified. At the sides and the top of the domain, symmetry boundary conditions are imposed (i.e. zero normal velocity and gradients). At the “walls”, the standard wall functions are used.

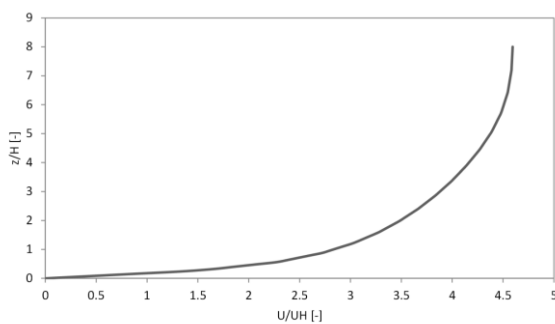


Figure 2. Log law profile of ratio of mean wind speed U to mean wind speed U_H at building height

4.3. CFD results and comparison with on-site measurements

The flow pattern and velocity distribution around the wind catcher model for prevailing wind directions of 90° are shown in figures 3 and 4. Figure 5 shows the air flow pattern through the tower shaft for three reference wind directions 330, 90 and 150. The down ward and upward air flow pattern (U_z) are indicated for the leeward and wind ward shafts at each wind direction.

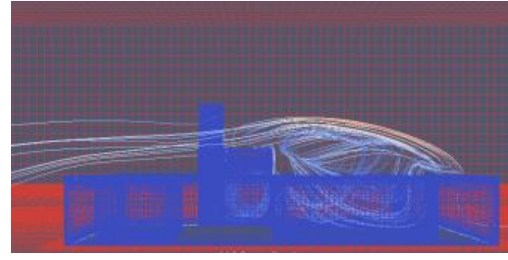


Figure 3. Flow pattern around wind catcher for prevailing wind directions of 90°

For validation purposes, the measured mean air velocity values are converted to velocity ratios by division by the reference wind speed (U_m/U_{ref}). The simulated velocity ratios are obtained by division of the simulated mean air velocity of each shaft by the simulated reference wind speed (U_{CFD}/U_{ref}).

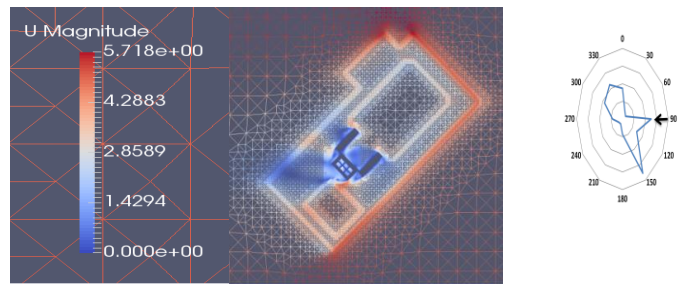


Figure 4. Top view of velocity distribution (U_{mag}) at experimental house position at height of 10 m for prevailing wind directions of 90° .

The simulation results have been compared with on-site wind speed measurements for the wind directions 330° , 90° and 150° (Figure 6). The average deviations for wind direction 90° in shafts B, D, E and A are 12.5%, 9.5%, 29.5% and 25.5%, respectively. A possible reason for this observation is that shaft B and D with low wind speed ratios are generally characterized by lower turbulence intensities and lower wind direction fluctuations, and can therefore be better described by the statistically steady RANS approach for the turbulent flow. The overall average deviation between simulated and measured wind speed was 19% for Standard $k-\epsilon$ model for wind direction 90° , which is considered a good agreement. Note that for the wind direction of 90° the wind ward shafts are shaft E and B providing downward flow behavior and Shaft A, shaft D considering the leeward shafts with upward flow pattern.

The overall average deviations in wind directions 330 and 150 are 48% and 45% respectively which at least partly caused by the deficiencies of steady RANS modelling and by neglecting the effect of buoyancy driven force. It should be mentioned that in this paper, an isothermal simulations are justified, in which mechanical turbulence generation dominates and thermal effects are absent.

5. CFD simulations: sensitivity analysis

To analyze the sensitivity of the results to geometrical and computational parameters [16], systematic changes are made to the reference wind tower case in one of the simulated wind direction $\theta = 90^\circ$.

5.1. Impact of grid resolution

Performing a grid-sensitivity analysis is important to reduce the discretization errors and the computational time. In this study, a grid-sensitivity analysis was performed based on three different grid resolutions near and inside the wind tower model. Coarsening and refining was performed in refinement box surrounding the wind tower shafts.

The results for mean velocity ratio (U_{mag}/U_{ref}) profiles along shaft A from the three different grid resolution, indicating only a very limited dependence of the results on the grid resolution. It can be indicated that the differences between grid 2 and grid 3 are significant,

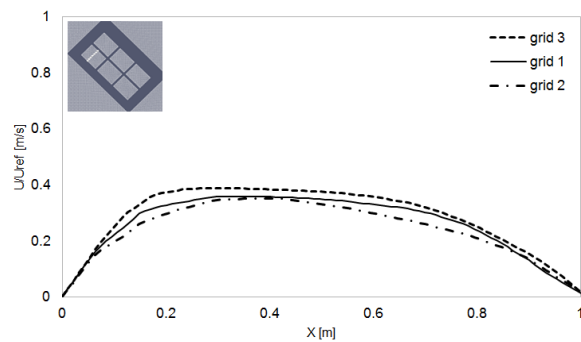


Figure 7. Comparison of mean velocity ratio (U_{mag}/U_{ref}) profiles along shaft A from the three different grid resolutions for wind direction 90°

whereas the differences between the grid 2 and grid 1 (final grid) are small. This seems to indicate that the grid 1 is a good compromise between computational accuracy and computational cost. This uniform grid is therefore selected for further analysis.

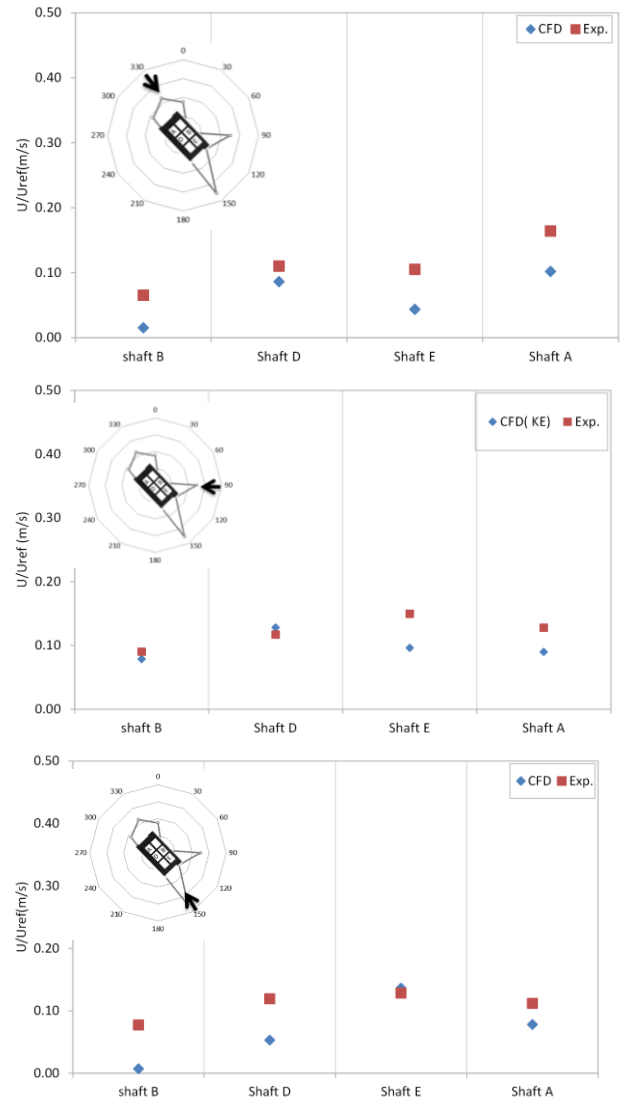


Figure 6. Comparison of mean velocity ratios by CFD simulation results and experimental measurements data in four tower shafts, for three prevailing wind directions 330 (top), 90 (middle), 150 (bottom)

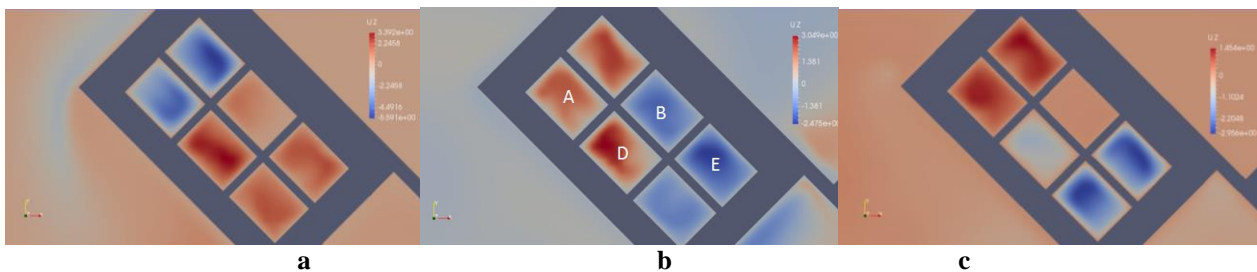


Figure 5. Air flow behavior inside four tower shafts ($H=6.35$ m) for three prevailing wind directions of 330 (a), 90 (b), 150 (c)

5.2. Impact of turbulence model

Isothermal 3D steady RANS simulations were made in combination with two turbulence models: the standard $k-\epsilon$ model ($Sk-\epsilon$) and the realizable $k-\epsilon$ model ($Rk-\epsilon$). The average and total deviations in four equipped tower shafts for each turbulence model, at the wind direction of 90° are given in "Table 1".

The differences between the standard $k-\epsilon$ model ($Sk-\epsilon$) and the realizable $k-\epsilon$ model ($Rk-\epsilon$) are most pronounced in shaft D, where the $Rk-\epsilon$ model tends to overestimate the velocity variations. The overall average deviation between simulated and measured wind speed was 19% for standard $k-\epsilon$ model and 30% for realizable $k-\epsilon$ model at wind direction of 90° . Hence the standard $k-\epsilon$ model generally provides an accurate results in four tower shafts at wind direction of 90° .

Table 1: The average absolute deviations for the equipped tower shafts for each turbulence model, for the wind direction of 90° .

Turbulenc e model	Shaf t B	Shaf t D	Shaf t E	Shaf t A	Total deviation (percentage)
Standard $k-\epsilon$	0.12	0.09	0.29	0.25	19%
Realizable $k-\epsilon$	0.25	0.13	0.45	0.40	30%

5. Thermal behaviour of wind catcher

To monitor the thermal behaviour of the reference wind catcher case during a hot summer day, the data from the temperature sensors was averaged over the warmest day of measuring period in shaft B (wind ward shaft) at wind direction 90° . Figure 8 shows the wind catcher plan and section and the position of the temperature sensors in Shaft B. Where the T_{out} is the ambient air temperature of 26th June 2015. T_1 and T_2 are coding as the surface temperature of the external and internal tower walls at the height of 10 m respectively. and T_3 as the surface temperature of the internal wall at height of 3m. T_{a1} is the air temperature (H=10m) and T_{a2} the air temperature at height 10m (the same height as the air velocity sensor height). The temperature data was recorded during the summer day at the warmest hour of day has shown in "Table 2".

Figure 9 shows the temperature difference between external and internal tower walls during a hot summer day on 26th June 2015. The temperature difference between the hot external surface and internal wall of the wind tower at 15 pm can explained by the high thermal inertia of the adobe walls. The amount of coolness which can be stored in the tower mass, due to the specific heat of the energy-storing material of the wind catcher walls to meet the cooling needs of the building during a hot summer day.

Figure 10 shows the temperature variation inside and through the tower shaft B comparing to the ambient air temperature. The results show the key role of tower walls to reduce the uncomfortable temperature fluctuations inside and through the wind catcher shafts. This phenomena can be seen in passive solar architecture by the use of massive walls which is called thermal flywheel effect. Based on the literature review, to achieve the desired time lag in the temperature at the inside surface of the massive wall

requires a very thick wall (typically 12-18"), and there is considerable attenuation in the temperature wave as it passes through the wall.

In present study the homogeneous adobe walls of the reference wind catcher case with the thickness of 14" and time lag of 24 hours, can significantly effect on lowering temperature of outlet air (T_{a2}) from the wind tower.

Figure 11 shows the wind and air velocity variations during a hot summer day which can provide a full analysis of the supply air from the tower during a hot summer day. The wind speed, wind direction and air velocity at 3 P.M. can be indicated from the daily data recorded on 26th June 2015. (Table 3)

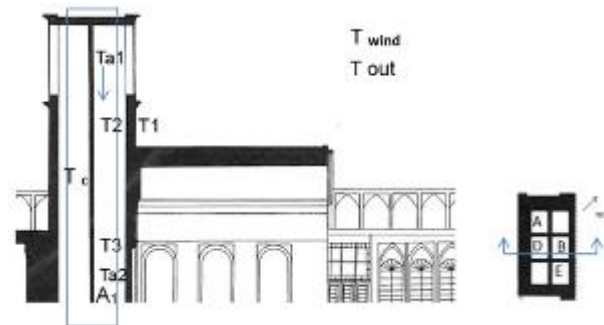


Figure 8. Wind catcher plan and the tower shafts coding (right), wind catcher section and the position of the temperature sensors (T_x) and air velocity sensor (A_1) in Shaft B (left)

Table 2: Temperature data from temperature sensors on a hot summer day (26th June 2015) at 15 pm.

Date/Time	T_{out} (°C)	T_{wind} (°C)	T_1 (°C)	T_2, T_3 (°C)	T_{a1} (°C)	T_{a2} (°C)
26th June 2015	45	43.9	55.6	40.1	39.8	39.2

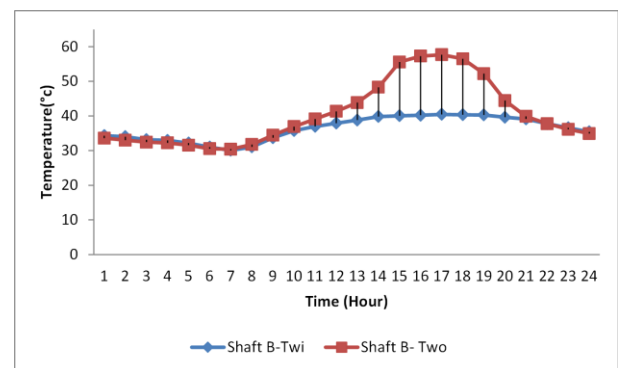


Figure 9. Temperature difference between external (T_1) and internal (T_2) tower walls during a hot summer day.

Table 3: wind and air velocity data on a hot summer day (26th June 2015) at 15 pm.

Date/Time	Wind speed (m/s)	Wind direction (°)	Air velocity (m/s)
26th June	1.5	90	0.85

Tables 2 and 3 show the supply air flow velocity of 0.85 m/s with the temperature of 39.2 °C in shaft B at 3 P.M. on 26th June 2016.

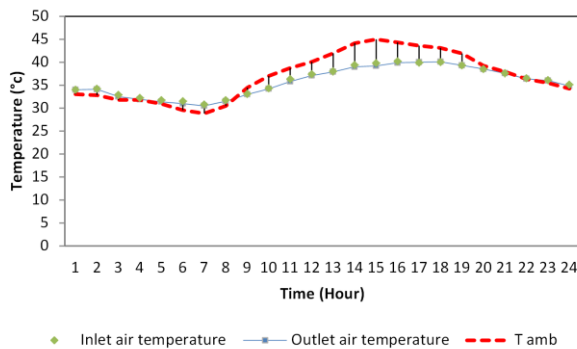


Figure 10. the temperature difference between the inlet air, outlet air and the ambient air during a hot summer day

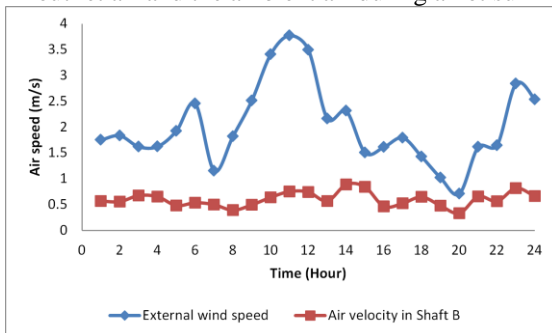


Figure 11. The wind and air velocity variations during a hot summer day (26th June 2015)

6. Conclusions

To analyze the wind and temperature behaviour of the wind catchers of Yazd city, a reference typical wind catcher case in city campus of Yazd university has been selected. The CFD simulation has been conducted to predict the air flow pattern around and through the wind catcher for three prevailing wind directions of 330°, 90°, 150° and an experimental analysis has been done to find the thermal behavior of tower in shaft B (windward shaft) at wind direction 90°. Based on the CFD simulation, this paper has presented a systematic evaluation of an isothermal 3D CFD for prediction of the air flow behavior of wind catchers of Yazd. The evaluation is based on a grid-sensitivity analysis and on validation with long-term full-scaled empirical measurements. The present study has shown that 3D steady RANS CFD, in spite of its limitations, is a suitable tool to predict the wind-driven flow behavior in wind towers. The impact of the turbulence model and suitable grid refinement has been investigated and it has been shown that a careful selection of these parameters is very important for accurate and reliable results. The basic OpenFoam CFD simulation template of wind-catcher reference case from the present paper easily allows future parametric studies to evaluate alternative design configurations of the wind catchers of Yazd city, especially when the different configurations are all a priori embedded within the same computational domain and grid. Considering that in this paper, isothermal CFD simulations are justified, in which mechanical turbulence generation dominates and thermal effects are small or absent. The deviation between the CFD and experimental

results at windward and leeward tower shafts can be explained due to the buoyancy and chimney effect and to the possibility of neglecting the effect of thermal modelling. Hence the impact of buoyancy-driven force in wind catcher CFD model should be considered and evaluated for future study. On the other hand, the thermal behavior of the wind catcher reference case has been analyzed experimentally during a hot summer day. The results reveal that the tower massive walls have a significant impact on the thermal behavior of the wind catcher due to their thermal properties in lowering air temperature (around 5.8 °C) leaving the tower during a hot summer day. At the final stage, the effect of both sun and wind simultaneously was evaluated on 26th June 2016. The study results show that the solar-wind catchers of Yazd city have a quiet effect in lowering air temperature and provide a comfort air velocity during a hot summer day without any energy cost.

References

- [1] AWS, 1997. Wind Resource Assessment Handbook: Fundamentals for Conducting a Successful Monitoring Program. Prepared for National Renewable Energy Laboratory.
- [2] Bahadori MN. 1985. "An improved design of wind towers for natural ventilation and passive cooling". *Solar Energy*; 35 (2): 119–129
- [3] Blocken, B., Carmeliet, J. 2002. "Spatial and temporal distribution of driving rain on a low-rise building". *Wind Struct.*; 5 (5): 441–462.
- [4] Blocken, B., Carmeliet, J. 2004b. "A review of wind-driven rain research in building science". *J. Wind Eng. Ind. Aerodyn.*; 92 (13): 1079–1130.
- [5] Blocken, B., Carmeliet, J., Stathopoulos, T. 2007. "CFD evaluation of wind speed conditions in passages between parallel buildings—effect of wall-function roughness modifications for the atmospheric boundary layer flow". *J. Wind Eng.*; 95 (9–11): 941–962.
- [6] Blocken, B., Carmeliet, J., Moonen, P., Stathopoulos, T. 2008. "A numerical study on the existence of the Venturi-effect in passages between perpendicular buildings". *Journal of Engineering Mechanics-ASCE*; 134 (12): 1021–1028.
- [7] Franke, J., Hellsten, A., Schlünzen, H., Carissimo, B. 2007. "Best practice guideline for the CFD simulation of flows in the urban environment". COST Action 732; COST Office: Brussels (Belgium).
- [8] Haw, L.C., O. Saadatian, M.Y. Sulaiman, S. Mat, and K. Sopian. (2012). Empirical Study of a wind-induced natural ventilation tower under hot and humid climatic conditions, *Energy and Buildings* 52: 28–38.
- [9] Hosseinnia, S.M., H. Saffari, and M. Ali Abdous. (2013). Effects of different internal designs of traditional wind towers on their thermal behavior, *Energy and Buildings* 62: 51–58.
- [10] Hedayat, Z.H., B. Belmans, H. Ayatollahi, I. Wouters, and F. Descamps. (2015 a). Performance assessment of ancient wind catchers -an experimental and analytical study. *Energy procedia*, 78: 2578 – 2583
- [11] Hedayat Z.H., N. Samkhaniani, B. Belmans, H. Ayatollahi, I. Wouters, and F. Descamps. (2015b). Energy modeling and air flow simulation of an ancient wind catcher in Yazd, 3rd International Congress on Civil Engineering, Architecture and Urban Development 29–31 December 2015, Shahid Beheshti University, Tehran, Iran.

- [12] Hedayat, Z.H., B. Belmans, H. Ayatollahi, I. Wouters, and F. Descamps, 2017 , Wind Energy and Natural Ventilation Potential of a Wind Catcher in Yazd–Iran (A Long-Term Measurement) .International Journal of Green Energy
- [13] Montazeri H. 2011.Experimental and numerical study on natural ventilation performance of various multi-opening wind catchers,Building and Environment;370–378.
- [14]OpenFOAM project web site, URL: <http://www.OpenFOAM.org>, OpenCFD Ltd.
- [15]Richards, P.J., Hoxey, R.P. 1993. “Appropriate boundary conditions for computational wind engineering models using the k-ε turbulence model”. J. Wind Eng. Ind. Aerodyn.; 46-47: 145-153.
- [16]Roache, P.J. 1998. Verification of codes and calculations. AIAA J.; 36: 696-702.
- [17] Schatzmann, M., Leidl, B., 2011. Issues with validation of urban flow and dispersion CFD models. J. Wind Eng. Ind. Aerodyn. 99 (4), 169e186.
- [18] van Hooff, T., Blocken, B., 2010a. Coupled urban wind flow and indoor natural ventilation modelling on a high-resolution grid: a case study for the Amsterdam ArenA stadium. Environ. Model. Softw. 25 (1), 51e65.
- [19] van Hooff, T., Blocken, B., 2010b. On the effect of wind direction and urban surroundings on natural ventilation of a large semi-enclosed stadium. Comput.Fluids39,1146e1155.
- [20] Yaghoubi MA , Sabzevari A , Golneshan AA. 1991. “Wind towers: measurement and performance”. SolarEnergy;47(2):97–106.